


Dynamical phase transition in the occupation fraction statistics for noncrossing Brownian particlesSoheli Mukherjee^{*} and Naftali R. Smith[†]*Department of Solar Energy and Environmental Physics, Blaustein Institutes for Desert Research,
Ben-Gurion University of the Negev, Sede Boqer Campus 8499000, Israel* (Received 10 April 2023; accepted 9 June 2023; published 26 June 2023)

We consider a system of N noncrossing Brownian particles in one dimension. We find the exact rate function that describes the long-time large deviation statistics of their occupation fraction in a finite interval in space. Remarkably, we find that, for any general $N \geq 2$, the system undergoes $N - 1$ dynamical phase transitions of second order. The $N - 1$ transitions are the boundaries of N phases that correspond to different numbers of particles which are in the vicinity of the interval throughout the dynamics. We achieve this by mapping the problem to that of finding the ground-state energy for N noninteracting spinless fermions in a square-well potential. The phases correspond to different numbers of single-body bound states for the quantum problem. We also study the process conditioned on a given occupation fraction and the large- N limiting behavior.

DOI: [10.1103/PhysRevE.107.064133](https://doi.org/10.1103/PhysRevE.107.064133)**I. INTRODUCTION**

Fluctuations in stochastic systems are of central importance in statistical mechanics and other fields [1–8]. Examples include population dynamics [4,8], nonequilibrium phase transitions [6], current statistics [1,2], condensation phenomena [5], etc., to name a few. In particular, large deviations (or rare events) have been a central theme of interest over the past few decades [9–15]. The fluctuations of the quantities of interest are encoded in the large deviation functions (LDFs), which are analogous to thermodynamic potentials in equilibrium systems [14]. One of the most remarkable phenomena in the context of large deviations is dynamical phase transitions (DPTs), which correspond to singularities (i.e., nonanalyticities) in LDFs [16–24].

The occupation (or residence) time of a particle is the time that it spends in some specified spatial domain. Fluctuations of the occupation time have been of interest in many random systems, including coarsening and phase ordering dynamics in magnetic systems [25–27], financial time series [28], and random walks on graphs [29,30]. Since the seminal work of Lévy [31], who computed the exact probability distribution of the occupation time for an ordinary Brownian motion, there have been studies of the fluctuations of occupation time for various processes in or out of equilibrium [32–46] because of their potential applications in many physical systems. For example, to analyze the morphological dynamics of interfaces [47], the fluorescence intermittency emitting from colloidal semiconductor dots [48], theory and experiments of blinking quantum dots [39], optical imaging [49], etc.

Recently, Tsobgni Nyawo and Touchette studied fluctuations of occupation fraction in a closed interval for a Brownian motion with and without drift [43,44]. They demon-

strated that this relatively simple model exhibits a DPT in the fluctuations of the occupation time in the presence of a drift in the long-time limit. Their analysis of this model used the Donsker-Varadhan (DV) large-deviation formalism [14,15,50–53], which maps the problem onto that of finding the ground-state energy of a quantum problem of a single particle inside an effective potential well. The transition occurs between the escape and confinement of the Brownian motion and is first order in nature. Similar DPTs have been observed in many systems in the limit of low noise and/or large system size [7,16–22,54,55]. To observe the DPT in a drifted Brownian motion occupation fraction, it is sufficient to consider the long-time limit without taking any additional limits of small or large parameters [43,44].

It is natural to ask how the occupation fraction fluctuates for $N > 1$ Brownian particles, conditioned not to cross each other (vicious Brownian motions). The noncrossing condition introduces correlations between the particles, making this a nontrivial, many-body problem. Since the pioneering works [56,57], noncrossing random walkers have been studied in the context of wetting and melting [57], networks of polymers [58], persistence properties in nonequilibrium systems [59], and more. Noncrossing Brownian motions are also known to be closely related to random matrix theory because the joint distribution of their positions (which has been studied in many contexts [60–66]) coincides, in some special cases, to that of eigenvalues of certain types of random matrices [67–69].

In this paper, we extend the study of occupation fraction statistics to $N > 1$ noncrossing Brownian particles in an interval $[-l, l]$ for a given time interval $[0, T]$. By extending the DV formalism to noncrossing Brownian motions, we study the LDF for all $N \geq 1$. We find that the DV formalism maps this problem to N noninteracting, spinless *fermions* in a square-well potential, cf. Refs. [64,65]. Interestingly, we find that the LDFs show multiple singularities: The system undergoes $N - 1$ second-order DPTs. These transitions are of very different nature to the DPT found for a single Brownian particle

^{*}soheli.mukherjee2@gmail.com[†]naftalismsith@gmail.com

in Refs. [43,44]. In particular, they occur in the absence of a drift, i.e., the dynamics obey time-reversal symmetry. In each of the N different phases, separated by the DPTs, a different number of particles remains in the vicinity of the interval for the entire dynamics, while the other particles wander away from the interval.

The paper is organized as follows. In Sec. II, we define the model and present the scaling behavior of the fluctuations of the occupation fraction. In Sec. III, we show how to extend the DV formalism to our system. In Sec. IV, we solve the DV problem and show that there are $N - 1$ second-order phase transitions. We give explicit results for $N = 2$. We also discuss the process conditioned on a given value of the occupation fraction, and some limiting behaviors that emerge in the limit $N \gg 1$. Finally, we summarize and conclude in Sec. V. Some details of the calculations are given in the Appendixes.

II. MODEL

We consider N one-dimensional Brownian particles, which are defined by the following stochastic differential equations:

$$\dot{X}_i(t) = \sqrt{2D} \xi_i(t), \quad i = 1, 2, \dots, N, \quad (1)$$

where X_i is the position of the i th particle, D is the diffusion constant, and $\xi_i(t)$ are Gaussian white noises with $\langle \xi_i(t) \rangle = 0$ and $\langle \xi_i(t) \xi_j(t') \rangle = \delta_{ij} \delta(t - t')$. Here $\langle \cdot \rangle$ denotes the ensemble average over realizations of the noise. We condition the particles to be noncrossing, i.e., $X_1(t) < X_2(t) < \dots < X_N(t)$ for all $t \in [0, T]$ [70].

The occupation fraction is defined as

$$\rho_T = \frac{1}{T} \int_0^T (\mathbb{1}_{[-l,l]}(X_1(t)) + \dots + \mathbb{1}_{[-l,l]}(X_N(t))) dt, \quad (2)$$

where $\mathbb{1}_{[-l,l]}(x)$ is the indicator function

$$\mathbb{1}_{[-l,l]}(x) = \begin{cases} 1, & \text{for } x \in [-l, l] \\ 0, & \text{otherwise.} \end{cases} \quad (3)$$

ρ_T is a random variable that takes values on $[0, N]$, where $\rho_T = 0$ ($\rho_T = N$) corresponds to realizations in which none (all) of the Brownian particles stay in the interval $[-l, l]$ for the entire duration of the dynamics. For $T \rightarrow \infty$, it becomes very unlikely for the Brownian particles to spend an extensive time $O(T)$ in the interval $[-l, l]$, so we expect that the probability distribution $P(\rho_T = \rho)$ concentrates around $\rho = 0$.

Rescaling space and time,

$$X/l \rightarrow X, \quad 2Dt/l^2 \rightarrow t, \quad (4)$$

Equations (1) and (2) become

$$\dot{X}_i(t) = \xi_i(t), \quad i = 1, 2, \dots, N \quad (5)$$

and

$$\rho_T = \frac{1}{T} \int_0^T (\mathbb{1}_{[-1,1]}(X_1(t)) + \dots + \mathbb{1}_{[-1,1]}(X_N(t))) dt, \quad (6)$$

with the rescaled T (which equals $2DT/l^2$ in the original variables). From this rescaling, it follows that the distribution of ρ_T takes the scaling form

$$P(\rho_T = \rho; D, l, T) = P\left(\rho_T = \rho; \frac{2DT}{l^2}\right) \quad (7)$$

in the original variables (where the dependence on the parameters is indicated explicitly, but will be suppressed for brevity below).

As we show below, in the long- T limit, the fluctuations of ρ_T follow the large deviation principle [9–15,50,51,71,72], which states that the probability distribution $P(\rho_T = \rho)$ scales as

$$P(\rho_T = \rho) \sim e^{-TI(\rho)}. \quad (8)$$

This describes an exponential decay with T at a rate described by the LDF or the rate function $I(\rho) \geq 0$, which is defined as

$$I(\rho) = -\lim_{T \rightarrow \infty} \frac{1}{T} \ln P(\rho_T = \rho). \quad (9)$$

(In the physical variables, this translates to $\mathcal{P}(\rho_T = \rho) \sim e^{-(2DT/l^2)I(\rho)}$, which is valid at $T \gg l^2/D$.)

In general, the rate function is difficult to calculate directly. However, according to the Gärtner-Ellis theorem [71,72], the rate function $I(\rho)$ can be calculated via the Legendre-Fenchel transform of the scaled cumulant generating function (SCGF), which is defined as [14,71,72]

$$\lambda(k) = \lim_{T \rightarrow \infty} \frac{1}{T} \ln \langle e^{T k \rho_T} \rangle. \quad (10)$$

The rate function is then expressed as the Legendre-Fenchel transformation of $\lambda(k)$,

$$I(\rho) = \sup_k \{k \rho - \lambda(k)\}, \quad (11)$$

provided that $\lambda(k)$ exists and differentiable [14]. If $\lambda(k)$ is convex, then the transform reduces to the Legendre transform, so the conjugate variable of k , ρ is given by [73]

$$\rho = \frac{d\lambda(k)}{dk}. \quad (12)$$

Hence, the problem reduces to that of calculating the SCGF of the occupation fraction of N noncrossing Brownian particles. In the next section, we explain how this can be done by extending the DV formalism to noncrossing Brownian particles.

III. DONSKER-VARADHAN FORMALISM

An equivalent description of the dynamics of the N Brownian particles is given in terms of the Fokker-Planck equation

$$\frac{\partial Q(X_1, \dots, X_N, t)}{\partial t} = L^\dagger Q(X_1, \dots, X_N, t). \quad (13)$$

Here $Q(X_1, \dots, X_N, t)$ is the unnormalized time dependent joint probability density function of the X_i 's, $L^\dagger = \frac{1}{2} \nabla^2$ is called the Fokker-Planck generator, with $\nabla^2 = \frac{\partial^2}{\partial X_1^2} + \dots + \frac{\partial^2}{\partial X_N^2}$. L^\dagger is a Hermitian operator ($L^\dagger = L$) as the dynamics have time-reversal symmetry [73]. Due to the noncrossing condition, we consider only the domain $X_1 < \dots < X_N$, with the Dirichlet boundary conditions:

$$Q(X_1, \dots, X_N, t)|_{X_i=X_{i+1}} = 0 \quad \text{for any } i \in \{1, \dots, N-1\}. \quad (14)$$

The *normalized* joint probability density function of X_1, \dots, X_N is

$$P(X_1, \dots, X_N, t) = \frac{Q(X_1, \dots, X_N, t)}{\mathcal{N}(t)}, \quad (15)$$

where $\mathcal{N}(t)$ is the (time-dependent) normalization constant:

$$\mathcal{N}(t) = \int_{-\infty}^{\infty} dX_1 \cdots \int_{-\infty}^{\infty} dX_N Q(X_1, \dots, X_N, t). \quad (16)$$

At long times, $t \rightarrow \infty$, $\mathcal{N}(t)$ goes as a power law $\mathcal{N}(t) \sim t^{-N(N-1)/4}$ [57,59,64,74,75].

A mathematical framework for calculating large deviations of time-averaged quantities in stochastic processes of the form Eq. (2) (which are often referred to as dynamical or additive observables) was formulated by Donsker and Varadhan in Refs. [50,51]. We will now extend this formalism to the case of noncrossing Brownian particles. To calculate $\lambda(k)$, the Feynman-Kac formula is used [32,53], which states that the evolution of the generating function of ρ_T involves a linear operator

$$\mathcal{L}_k = \frac{1}{2} \nabla^2 + k(\mathbb{1}_{[-1,1]}(X_1) + \cdots + \mathbb{1}_{[-1,1]}(X_N)), \quad (17)$$

which is called the tilted generator. The SCGF of ρ_T is evaluated as the largest eigenvalue of \mathcal{L}_k [76] (see Appendix A for more detailed calculation)

The eigenvalue problem is defined by the equation

$$\mathcal{L}_k r_k(X_1, \dots, X_N) = \lambda(k) r_k(X_1, \dots, X_N), \quad (18)$$

where $r_k(X_1, \dots, X_N)$ is the right eigenfunction of \mathcal{L}_k , together with the same boundary conditions as for Q , i.e.,

$$r(X_1, \dots, X_N, t)|_{X_i=X_{i+1}} = 0 \text{ for any } i \in \{1, \dots, N-1\}. \quad (19)$$

Note that as the operator \mathcal{L}_k is Hermitian, its left eigenfunctions are the same as $r_k(X_1, \dots, X_N)$. We are generally interested in normalizable solutions, and we (arbitrarily) choose the normalization constant to be 1:

$$\int_{-\infty}^{\infty} dX_1 \cdots \int_{-\infty}^{\infty} dX_N |r_k(X_1, \dots, X_N)|^2 = 1. \quad (20)$$

Equation (18) with the tilted operator (17) and the boundary condition (19) can be recognized as the time-independent Schrödinger equation of N noninteracting, spinless fermions up to an overall minus sign with $\frac{\hbar^2}{2m} = \frac{1}{2}$ in a finite potential well:

$$V_k(x) = -k\mathbb{1}_{[-1,1]}(x). \quad (21)$$

Figure 1 shows a schematic plot of the equivalent quantum problem. This implies that the $\lambda(k)$ equals minus the (many-body) ground-state energy of $-\mathcal{L}_k$. For $N = 1$, the problem reduces to that of a single particle in the potential well V_k , which was solved in Refs. [43,44].

IV. RESULTS

The SCGF $\lambda(k)$ for general N is calculated from the ground-state energy of N noninteracting, spinless fermions in a square well potential of depth k , which is given by the sum of the single-body energy levels. For a single Brownian particle ($N = 1$), there is always a bound state for any $k > 0$ given by the cosine inside the well and two decaying exponentials outside the well. The single-body energy levels of a quantum particle inside a square-well potential can be found in any standard textbook of quantum physics [77,78], and each of them is given by the solution to one of two transcendental

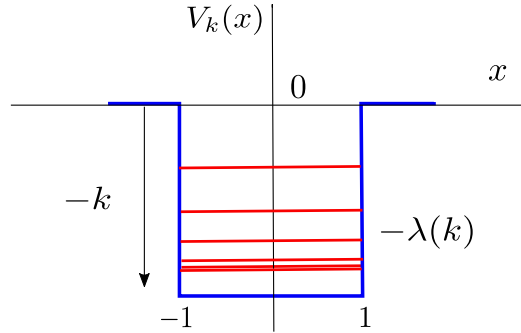


FIG. 1. The effective quantum problem of N fermions in a square potential well (21) of depth $-k$, whose solution yields the behavior of fluctuations of the occupation fraction in the interval $[-1, 1]$ of N noncrossing Brownian particles. The solid red lines represent the single-particle energy levels occupied by the fermions. $-\lambda(k)$ is the many-body ground-state energy.

equations (see below). For any general N , an interesting effect occurs: As k is increased, the number of solutions to the transcendental equations increases and, as shown below, this results in $N - 1$ DPTs which correspond to critical values of k .

In this section, we first briefly recall the single-body energy levels of a quantum particle in a finite potential well. Then, we give a brief review of the results for the case $N = 1$ [43,44]. Next, we study the problem for general N , giving explicit results for the case $N = 2$ which is already sufficient to observe the DPT. We then consider the large- N limit where we uncover a universal behavior of the system. We also discuss the conditioned process, both for general N and in the large- N limit.

A. Single-body energy levels

Due to the symmetry in the potential Eq. (21), the single-body wave functions of bound states are either symmetric or antisymmetric. For any $k > 0$, there always exists at least one bound state with a symmetric wave function [78]. As the depth of the potential k increases, the number of bound energy levels increases, with the wave functions alternating between symmetric and antisymmetric. The energy levels $-\lambda_1, -\lambda_2, \dots$ satisfy the following transcendental equations [77,78]:

$$A + A \tan^2(\sqrt{2A}) = k \quad \text{for symmetric case} \quad (22)$$

and

$$A + A \cot^2(\sqrt{2A}) = k \quad \text{for antisymmetric case}, \quad (23)$$

where

$$A = k - \lambda_i(k). \quad (24)$$

The i th energy level ($i = 1, 2, \dots$) is the solution of Eq. (22) (for odd i) or Eq. (23) (for even i) for the following range of A 's:

$$\frac{\pi^2}{8}(i-1)^2 < A_i < \frac{\pi^2}{8}i^2. \quad (25)$$

B. $N = 1$

For a single ($N = 1$) Brownian motion, the problem was solved in Refs. [43,44]. The calculation of $\lambda(k) = \lambda_1(k)$ boils down to calculating the ground-state energy of one quantum particle trapped in a potential well with depth k . The ground-state wave function is symmetric, satisfying Eq. (22), where $0 \leq k < \infty$ and $0 \leq A \leq \frac{\pi^2}{8}$. Eqs. (22) and (24) thus give $\lambda(k)$ in a parametric form (with k and λ both given explicitly as functions of the parameter A).

The conjugate variable ρ and the rate function $I(\rho)$ of the problem can also be expressed in terms of the variable A , thus giving the rate function in a parametric form:

$$\rho = \frac{d\lambda}{dk} = \frac{d\lambda/dA}{dk/dA} = 1 - \frac{\cos^2(\sqrt{2A})}{1 + \sqrt{2A} \tan(\sqrt{2A})}, \quad (26)$$

$$I = \rho k - \lambda = \frac{A\sqrt{2A} \tan(\sqrt{2A})}{\sqrt{2A} \tan(\sqrt{2A}) + 1}. \quad (27)$$

The asymptotic behaviors of $\lambda(k)$ and $I(\rho)$ are given by Ref. [44] (see also Appendix B for a derivation):

$$\lambda(k) \simeq \begin{cases} 2k^2, & k \rightarrow 0 \\ k - \frac{\pi^2}{8} + \frac{\pi^2}{4\sqrt{2k}}, & k \rightarrow \infty, \end{cases} \quad (28)$$

$$I(\rho) \simeq \begin{cases} \frac{\rho^2}{8}, & \rho \rightarrow 0 \\ \frac{\pi^2}{8} - 3\left(\frac{\pi^2}{8\sqrt{2}}\right)^{2/3} (1 - \rho)^{1/3}, & \rho \rightarrow 1. \end{cases} \quad (29)$$

The SCGF and rate function for $N = 1$ are shown in Figs. 2 and 3, respectively [$\lambda_1(k)$ and $I_1(\rho)$, respectively].

C. General N

For $N > 1$, the problem is mapped to N noninteracting, spinless fermions in the potential well (21). As k is increased, the number of single-body bound states increases and the fermions alternately occupy the odd and even energy levels which are found from Eqs. (22) and (23), respectively. These energy levels correspond to multiple values of A with ranges given by Eq. (25).

Importantly, there are $N - 1$ critical values of $k = k_{c,i} \equiv i^2 \frac{\pi^2}{8}$ for $i \in \{1, \dots, N - 1\}$, at which the number of bound states increases. The critical values correspond to singularities of $\lambda(k)$ and these correspond to DPTs, i.e., singularities of $I(\rho)$. Indeed, at k slightly larger than $k_{c,i}$, $\lambda_{i+1}(k)$ behaves asymptotically as (for details, see Appendix B)

$$\lambda_{i+1}(k) \simeq \frac{1}{2}(k - k_{c,i})^2 \quad (30)$$

and, as a result, the SCGF $\lambda(k)$ shows a jump in the second derivative at $k = k_{c,i}$. As we show below, this leads to a jump in the second derivative of $I(\rho)$, which we interpret as a second-order DPT (see next subsection for details of the particular case $N = 2$).

For $k < k_{c,N-1}$, $\lambda(k) = \lambda_1(k) + \dots + \lambda_M(k)$, where M is the number of single-body bound states. The eigenfunction $r_k(X_1, \dots, X_N)$ in Eq. (18) is now given by the following Slater determinant [79]:

$$\Psi(X_1, \dots, X_N) = \begin{vmatrix} \psi_1(X_1) & \dots & \psi_N(X_1) \\ \vdots & \ddots & \vdots \\ \psi_1(X_N) & \dots & \psi_N(X_N) \end{vmatrix}, \quad (31)$$

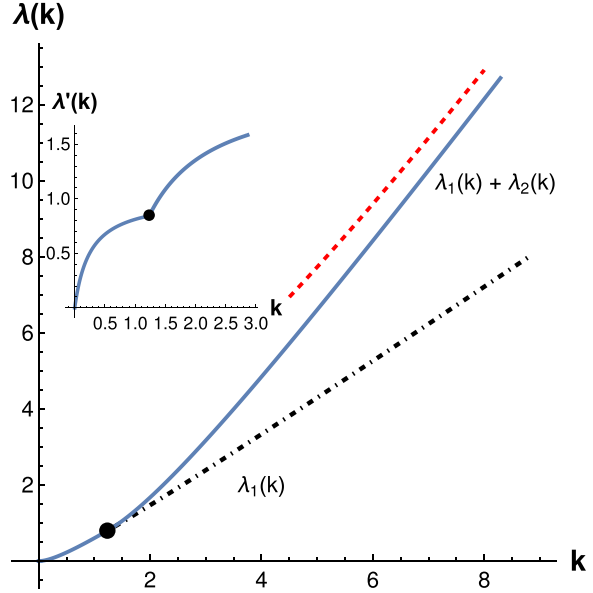


FIG. 2. Solid line: The plot of the exact SCGF $\lambda(k)$ as a function of k for $N = 2$ noncrossing Brownian particle occupation fraction. The solid circle represents the critical point $k_c = \pi^2/8$. For $k < k_c$, $\lambda(k)$ coincides with the SCGF $\lambda_1(k)$ for $N = 1$, and for $k > k_c$, the SCGF is $\lambda(k) = \lambda_1(k) + \lambda_2(k)$, where $-\lambda_2(k)$ is the energy of the first excited state for the potential (21). The dot-dashed line represents the continuation of the single particle SCGF for $k > k_c$. The red dashed line depicts the asymptotic behavior of $\lambda(k)$ for $k \gg 1$. The second derivative of $\lambda(k)$ has a jump discontinuity at $k = k_c$. This can be seen as a corner singularity in the inset, which shows $d^2\lambda/dk^2$ as a function of k .

where $\psi_j(X_i)$ is the single particle state function. For $k < k_{c,N-1}$, $M < N$, so the many-body energy spectrum is continuous, and $N - M$ of the fermions will not be localized around the interval $[-1, 1]$. As we show below, the interpretation of this in terms of the original problem is that M of the Brownian particles remain in the vicinity of the interval $[-1, 1]$ and the remaining $N - M$ particles do not.

In the next subsection, we will analyze the results for a fixed N . We consider the occupation fraction for $N = 2$ noncrossing Brownian particles, as it displays all of the interesting features for any general N .

D. $N = 2$

For $N = 2$, the two lowest single-body energy levels are found from Eqs. (22) and (23), which together take the form

$$k = A_2(1 + \cot^2 \sqrt{2A_2}) = A_1(1 + \tan^2 \sqrt{2A_1}). \quad (32)$$

There is a critical value of $k = k_c \equiv k_{c,1} = \frac{\pi^2}{8}$ (corresponds to $A_1 = 0.436191\dots$ and $A_2 = \frac{\pi^2}{8}$), below which only one physically possible solution A_1 contributes, whereas for $k > k_c$, the $\lambda_2(k)$ (corresponding to the solution A_2) contributes and the total SCGF of the problem is

$$\lambda(k) = \lambda_1(k) + \lambda_2(k). \quad (33)$$

Figure 2 shows the plot of the SCGF for the two noncrossing Brownian particle occupation fractions (shown by the solid

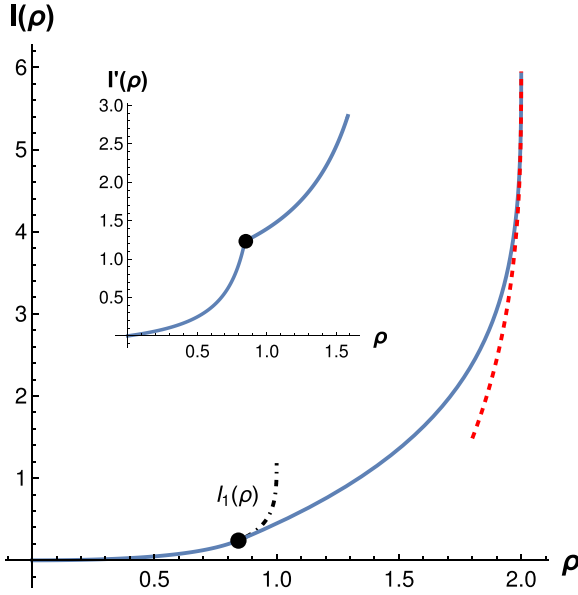


FIG. 3. Solid line: The plot of the exact rate function $I(\rho)$ as a function of the occupation fraction ρ for $N = 2$ noncrossing Brownian particles. The solid circle represents the critical point $\rho_c = 0.84375 \dots$. For $\rho < \rho_c$, the rate function coincides with the rate function for the corresponding single particle problem ($N = 1$). The dot-dashed line represents the continuation of the single-particle rate function for $\rho > \rho_c$. The red dashed line depicts the asymptotic behavior of $I(\rho)$ for $\rho \rightarrow 2$. The second derivative of $I(\rho)$ has a jump discontinuity at $\rho = \rho_c$, which we interpret as a second-order DPT. This can be seen as a corner singularity in the inset, which shows $dI/d\rho$.

line). For $k < k_c$, the SCGF coincides with $\lambda_1(k)$. At $k = k_c$, $\lambda_2(k)$ starts to contribute and continues to exist with $\lambda_1(k)$ for all $k > k_c$.

Similarly, for the rate function, there is a critical value of the occupation fraction $\rho = \rho_c = \lambda'_1(k_c) = 0.84375 \dots$, below which the rate function coincides with the rate function $I_1(\rho)$ of the case $N = 1$. For $\rho > \rho_c$, the rate function is given by the Legendre transform of the SCGF $\lambda_1(k) + \lambda_2(k)$. Figure 3 shows the plot of the rate function for $N = 2$.

Next, we study the asymptotic behaviors of the SCGF, with particular emphasis on the behavior near the critical point $k \rightarrow k_c$ ($\rho \rightarrow \rho_c$), where we study the DPT in detail.

In the $k \rightarrow 0$ limit, which corresponds to $\rho \rightarrow 0$, the SCGF and the rate function coincide with their counterparts for $N = 1$, and their asymptotic behaviors in these limits are given by the first lines of Eqs. (28) and (29), respectively.

In the critical regime, the SCGF behaves as

$$\lambda(k) \simeq \begin{cases} \lambda_1(k), & k < k_c \\ \lambda_1(k) + \frac{1}{2}(k - k_c)^2, & k - k_c \ll k_c. \end{cases} \quad (34)$$

Similarly, the rate function near ρ_c behaves as

$$I(\rho) \simeq \begin{cases} I_1(\rho), & \rho < \rho_c \\ I_1(\rho_c) + k_c(\rho - \rho_c) + B(\rho - \rho_c)^2, & \rho - \rho_c \ll \rho_c. \end{cases} \quad (35)$$

where $B = \frac{1}{2[\lambda''_1(k_c)+1]} \simeq 0.447705 \dots$. The detailed calculations are presented in Appendix B.

Clearly, the second derivative of the SCGF jumps at the critical point. As we now show, the same is true for the rate function. The first derivative of the rate function $I(\rho)$ is continuous because $I'_1(\rho_c) = k_c$, but $I'(\rho)$ shows a corner singularity as shown in the bottom inset of Fig. 3. Indeed, the second derivative shows a jump discontinuity (see Appendix B)

$$I''(\rho) \simeq \begin{cases} I''_1(\rho) = \frac{1}{\lambda'_1(k)} & \rho < \rho_c \\ 2B & \rho - \rho_c \ll \rho_c. \end{cases} \quad (36)$$

We interpret the jump in the second derivative of I as a DPT of second order [21,22].

In the $k \rightarrow \infty$ limit, the SCGF behaves as

$$\lambda(k) \simeq 2k - \frac{5\pi^2}{8} + \frac{5\pi^2}{4} \frac{1}{\sqrt{2k}}. \quad (37)$$

Taking the Legendre transform of this expression, we find that the corresponding limit $\rho \rightarrow 2$ of the rate function behaves as

$$I(\rho) \simeq \frac{5\pi^2}{8} - 3 \left(\frac{5\pi^2}{8\sqrt{2}} \right)^{2/3} (2 - \rho)^{1/3}. \quad (38)$$

The details of the calculations are given in Appendix B. The asymptotic behaviors of the SCGF and the rate function are shown in Figs. 2 and 3, respectively, by the dashed red lines.

E. Large N behavior

Let us consider the large- N limit, where, as we show below, a universal behavior emerges at $\rho \gg 1$. This corresponds to $k \rightarrow \infty$, where the single-body energy levels can be approximated as the energy levels of particle in a box, i.e., $E_i \simeq -k + \frac{\pi^2}{8} i^2$. $-\lambda(k)$ for the large N limit is thus the sum of the energy levels up to M , where M is the energy level at which $E_M \simeq 0$, which gives

$$M \simeq \frac{2\sqrt{2k}}{\pi}. \quad (39)$$

Thus, the SCGF can be written as

$$\begin{aligned} \lambda(k) &= -(E_1 + E_2 + \dots + E_M) \\ &\simeq Mk - \frac{\pi^2}{24} M^3 \simeq \frac{4\sqrt{2}}{3\pi} k^{3/2}. \end{aligned} \quad (40)$$

Taking the Legendre transform, we obtain

$$I(\rho) \simeq \frac{\pi^2}{24} \rho^3. \quad (41)$$

Equation (41) is valid in the limit $1 \ll \rho < N$. Despite the fact that $I(\rho)$ has $N - 1$ singularities, we find that the limiting behavior (41) is nevertheless smooth. Figure 4 shows the exact SCGF and rate function together with the limiting behaviors for $N = 5$, which turns out to be large enough to observe excellent agreement. There are four critical points at which the DPTs of second order occur.

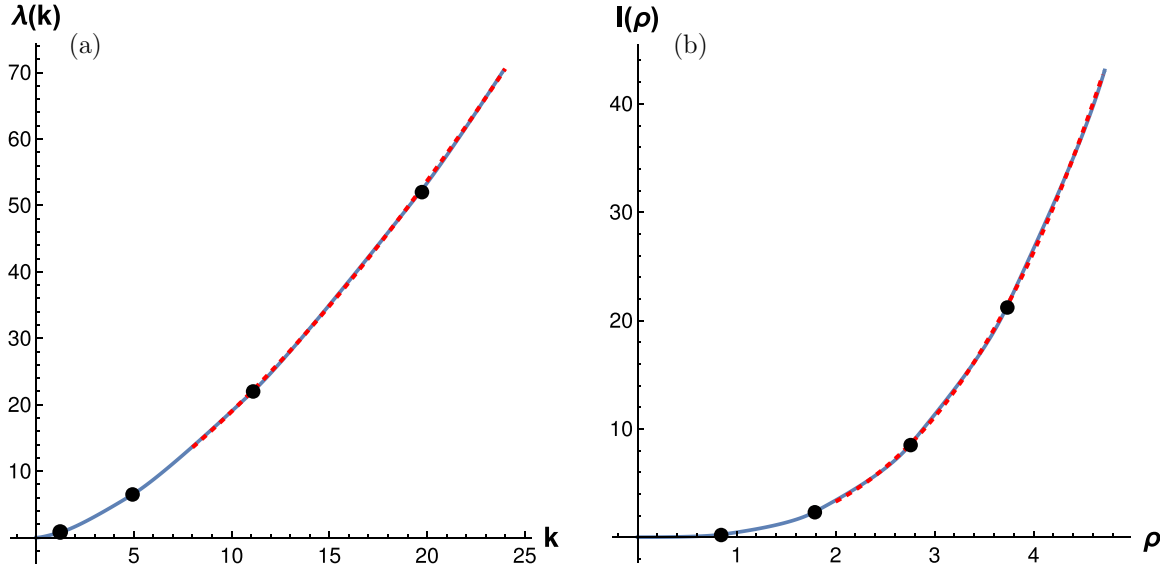


FIG. 4. The plot of the (a) SCGF as a function of k and (b) rate function as a function of ρ for $N = 5$ Brownian particles. There are four critical points where the second-order DPTs happen, shown by black dots. The red dashed lines depict the asymptotic large- k and large- ρ behaviors, see Eqs. (40) and (41). The exact and asymptotic expressions agree surprisingly well (blue) and are indistinguishable at the scale of the figure.

F. Conditioned process

$|\Psi(X_1, \dots, X_N)|^2$ is the joint distribution of the positions of the particles at some intermediate time $0 < t < T$ conditioned on a given value of ρ [44]. Therefore, the N phases correspond to conditioned processes in which M particles stay in the vicinity of the interval $[-1, 1]$ (where $M = 1, \dots, N$). It is then intriguing to study the properties of the conditioned process in more detail. This can be done by exploiting the interpretation of the joint distribution as that of the positions of M noninteracting fermions confined by the potential $V_k(x)$. The latter system is closely related to that which was studied in Ref. [80]. Below, we reiterate some of the main properties, but we refer the reader to Ref. [80] for details.

Quantum fluctuations of interacting or noninteracting fermions, possibly confined by an external potential, have attracted much recent attention [81–85], in particular, due to their importance in applications such as experiments in cold atoms [86–91]. Using a variety of analytical methods, such as determinantal processes and surprising connections to random matrix theory [80,83–85,92–94], fundamental properties such as the spatial density of fermions and its correlations have been studied. For M noninteracting fermions in the presence of a trapping potential at zero temperature (i.e., in the many-body ground state), the quantum correlations are encoded in a fundamental object called the kernel, that is given by

$$K_M(x, y) = \sum_{j=1}^M \psi_j^*(x) \psi_j(y), \quad (42)$$

where $\psi_1(x), \dots, \psi_M(x)$ are the wave functions of the M single-body lowest energy states. The quantum correlations of the fermions' positions can be expressed using the kernel. For instance, the density of particles at point x is given by $\mathcal{R}_M(x) = K_M(x, x)$, see, e.g., Ref. [85] for more details.

The above expressions for \mathcal{R}_M and K_M are valid for arbitrary M , and (for the potential $V(x) = V_k(x)$) they describe the density and density-density correlations of the M particles that remain near the interval $[-1, 1]$, conditioned on a given value of the occupation fraction. However, in the large- M limit they approach universal behaviors as we now describe. Over large scales, the density is in general given by the local density (or Thomas-Fermi) approximation, $\mathcal{R}_M(x) \simeq k_F(x)/\pi$, where $k_F(x) \simeq \sqrt{2(\mu - V(x))}$ is the local Fermi wave vector and μ is the Fermi energy (we consider $\hbar = m = 1$). The density is normalized such that $\int_{-\infty}^{\infty} \mathcal{R}_M(x) dx = M$. For the square-well potential $V_k(x)$, as we saw above, M is determined by the condition $\mu = E_M \simeq 0$, so we obtain

$$\mathcal{R}_M(x) \simeq \begin{cases} \sqrt{2k}/\pi \simeq M/2, & x \in [-1, 1] \\ 0, & x \notin [-1, 1], \end{cases} \quad (43)$$

which thus determines $M \simeq 2\sqrt{2k}/\pi$ in agreement with Eq. (39) above. This gives the mean interparticle distance between particles inside the interval, $d = 1/\mathcal{R}_M(x) = 2/M$. Moreover, the density correlations inside the interval are given in terms of the celebrated sine kernel [83,85,93]:

$$K_M(x, y) \simeq \frac{\sin[k_F(x)(x - y)]}{\pi(x - y)}. \quad (44)$$

These expressions for the density and the kernel break down near the edges of the interval, $x = \pm 1$. In fact, the behavior of a noninteracting Fermi gas in the presence of a step-function potential was analyzed in Ref. [80] in some detail. A universal form of the density and kernel were obtained. For $\mu \simeq 0$ (the so-called critical case), they are given by

$$\mathcal{R}_M(x) \simeq \frac{1}{d} n_c\left(\frac{x}{d}\right), \quad K_M(x, y) \simeq \frac{1}{d} \kappa_c\left(\frac{x}{d}, \frac{y}{d}\right), \quad (45)$$

respectively, where the universal functions n_c and κ_c are given explicitly in Ref. [80]. They provide an interpolation of \mathcal{R}_M

and K_M between the regime inside the interval ($x \in [-1, 1]$) and outside it ($x \notin [-1, 1]$).

V. DISCUSSION

We have studied the fluctuations of the occupation fraction of N noncrossing Brownian particles in a finite interval. We found that the rate function that describes these fluctuations at long times undergoes a sequence of $N - 1$ DPTs of second order. The N different phases correspond to different numbers of particles in the vicinity of the interval. We achieved this by extending the DV formalism to noncrossing Brownian particles and found that this maps the problem to that of N noninteracting spinless fermions in the presence of an effective potential. Under this mapping, the N phases correspond to different numbers of bound single-body states of the effective potential.

This DPT observed here for any $N \geq 2$ is of very different nature to the DPT that has been previously found for a single particle ($N = 1$). The latter DPT only occurs if the particle experiences an additional external drift (which leads to breaking of time-reversal symmetry) [43,44], and its properties are quite different to those of the DPTs that we found here. For instance, it involves coexistence between two different phases, which correspond to the particle being confined (or not) to the vicinity of the interval. However, in the present work, we have found $N - 1$ DPTs that separate between N temporally homogeneous phases, each corresponding to a different number of particles which are in the vicinity of the given interval for the entire dynamics.

It would be interesting to study fluctuations of the occupation time in presence of other interactions between the Brownian particles (instead of or in addition to the noncrossing condition). This problem has been solved in the limit $N \gg 1$ for a broad class of interacting diffusive gases (e.g., the exclusion process, that does not include the gas of noncrossing Brownian particles as a particular case, in Ref. [45]). Another natural extension of the present problem would be to study the effect of a drift in the system or to study the occupation time for other processes, such as fractional Brownian motion or for active particles. Moreover, one could study more detailed quantities such as the empirical distribution of the positions of the particles.

ACKNOWLEDGMENT

We acknowledge several useful discussions with Pierre Le Doussal on related topics.

APPENDIX A: DONSKER-VARADHAN FORMALISM FOR NONCROSSING PARTICLES

We first consider the unnormalized joint probability distribution $Q(X_1, \dots, X_N, \mathcal{R}, t)$ of the X_i 's and $\mathcal{R} = t\rho_t$. Q satisfies the Fokker-Planck equation

$$\frac{\partial Q}{\partial t} = L^\dagger Q - \mathbb{1}_{[-1,1]}(x) \frac{\partial Q}{\partial \mathcal{R}} \tag{A1}$$

together with the noncrossing boundary conditions given in Eq. (14) at $X_i = X_{i+1}$. It is convenient to define the generating

function:

$$G_k(X_1, \dots, X_N, t) = \int e^{k\mathcal{R}} Q(X_1, \dots, X_N, \mathcal{R}, t) d\mathcal{R}. \tag{A2}$$

According to Feynman-Kac formula [32,53], G_k evolves with time as

$$\frac{\partial G_k(X_1, \dots, X_N, t)}{\partial t} = \mathcal{L}_k G_k(X_1, \dots, X_N, t), \tag{A3}$$

where

$$\mathcal{L}_k = L + k\mathbb{1}_{[-1,1]}(x), \tag{A4}$$

known as the tilted generator. Note that G_k also satisfies the boundary conditions (14).

Equation (A3) can be solved by expanding G_k over the eigenbasis of \mathcal{L}_k [95],

$$G_k(X_1, \dots, X_N, t) = \sum_i c_i e^{t\zeta_i} r_k^i(X_1, \dots, X_N), \tag{A5}$$

where ζ_i and $r_k^i(X_1, \dots, X_N)$ are the eigenvalues and eigenfunctions of \mathcal{L}_k respectively, and the c_i 's are coefficients that depend on the initial condition.

For $T \rightarrow \infty$, the sum in Eq. (A5) is dominated by the largest eigenvalue ζ_{\max} (and if ζ_{\max} doesn't exist, then instead we must use the supremum of the ζ_i 's). In this long-time limit, the normalization factor $\mathcal{N}(t)$ goes as a power law $\mathcal{N}(t) \sim t^{-N(N-1)/4}$ [57,59,64,74,75]. Comparing Eq. (A5) to the definition of the SCGF in Eq. (10), it can be concluded that $\lambda(k) = \zeta_{\max}$, as the logarithm of $\mathcal{N}(t)$ can be neglected.

APPENDIX B: ASYMPTOTIC BEHAVIORS OF $\lambda(k)$ AND OF $I(\rho)$

In this Appendix, we show the details of the calculation of some of the asymptotic behaviors of the SCGF and the rate function. We mostly focus on the case $N = 2$, and consider the limits $k \rightarrow 0$ ($\rho \rightarrow 0$), $k \rightarrow \infty$ ($\rho \rightarrow 2$), and near the critical point, $k \simeq k_c$. We use Eqs. (22)–(24) to study the asymptotic behaviors for different limits of A (or k).

1. $k \simeq k_c$

For any general N , for k , that is near the critical point $k_{c,i} = \frac{i^2\pi^2}{8}$ but slightly larger (i.e., for $k > k_{c,i}$ with $k - k_{c,i} \ll k_{c,i}$), using $\tan x = \tan(x - n\pi) \simeq x - n\pi$ (for even i) and $\cot x = \cot(x - n\pi) \simeq x - n\pi$ (for odd i) for $x \simeq n\pi$, the k and $\lambda_{i+1}(k)$ behaves for $A_i \rightarrow \frac{i^2\pi^2}{8}$ as Eq. (22) becomes

$$k \simeq \frac{1}{2} \left(\frac{i^2\pi^2}{8} - A_i \right)^2 + A_i, \tag{B1}$$

leading to

$$\begin{aligned} \lambda_{i+1}(k) = k - A_i &\simeq \frac{1}{2} \left(\frac{i^2\pi^2}{8} - A_i \right)^2 \\ &\simeq \frac{1}{2} \left(k - \frac{i^2\pi^2}{8} \right)^2, \end{aligned} \tag{B2}$$

which coincides with Eq. (30) of the main text. Using the above two equations, the behavior of the SCGF $\lambda(k)$ for

$N = 2$ can now be written as

$$\lambda(k) \simeq \lambda_1(k) + \frac{1}{2}(k - k_c)^2, \quad (\text{B3})$$

which is Eq. (34) in Sec. IV. Taking the derivative, we have

$$\rho = \frac{d\lambda}{dk} \simeq \lambda'_1(k) + (k - k_c) \simeq \rho_c + [\lambda''_1(k_c) + 1](k - k_c), \quad (\text{B4})$$

where we used $\rho_c = \lambda'_1(k_c)$. Inverting this relation, we obtain

$$k \simeq k_c + \frac{\rho - \rho_c}{\lambda''_1(k_c) + 1}. \quad (\text{B5})$$

Taking the Legendre transform of the Eq. (34) while using Eqs. (B4) and (B5), the expression of the rate function at ρ that is slightly larger than ρ_c can now be expressed as

$$I(\rho) \simeq I_1(\rho_c) + k_c(\rho - \rho_c) + \frac{1}{2[\lambda''_1(k_c) + 1]}(\rho - \rho_c)^2, \quad (\text{B6})$$

which coincides with the second line of Eq. (35) in Sec. IV.

2. $k \rightarrow 0$

In the $k \rightarrow 0$ limit, the SCGF $\lambda(k) = \lambda_1(k) \approx 0$, which implies $A \rightarrow 0$. Around $A = 0$, using Eqs. (22) and (24), the asymptotic behaviors of $\lambda(k)$ and k are

$$\lambda(k) \simeq 2A^2, \quad k \simeq A + 2A^2, \quad (\text{B7})$$

respectively. This implies

$$\lambda(k) \simeq 2k^2, \quad (\text{B8})$$

coinciding with the first line of Eq. (28) in Sec. IV. The Legendre transform of $\lambda(k)$ in this limit is thus

$$I(\rho) \simeq \frac{\rho^2}{8}, \quad (\text{B9})$$

which coincides the first line of Eq. (29) in Sec. IV.

3. $k \rightarrow \infty$

In the limit $k \rightarrow \infty$, A_1 goes as $A_1 \rightarrow \frac{\pi^2}{8}$. Considering Eq. (22), the asymptotic behavior of the left-hand side of Eq. (22), near this value of A_1 we obtain

$$k \simeq \frac{\pi^4}{32\left(\frac{\pi^2}{8} - A_1\right)^2} - \frac{3\pi^2}{8\left(\frac{\pi^2}{8} - A_1\right)} + \frac{1}{24}(21 + \pi^2) - \left(\frac{1}{3} - \frac{1}{2\pi^2}\right)\left(\frac{\pi^2}{8} - A_1\right), \quad (\text{B10})$$

which yields

$$\begin{aligned} \lambda_1(k) &= k - A_1 \\ &\simeq \frac{\pi^4}{32\left(\frac{\pi^2}{8} - A_1\right)^2} - \frac{3\pi^2}{8\left(\frac{\pi^2}{8} - A_1\right)} - \frac{\pi^2}{12} + \frac{7}{8} \\ &\quad + \left(\frac{2}{3} + \frac{1}{2\pi^2}\right)\left(\frac{\pi^2}{8} - A_1\right). \end{aligned} \quad (\text{B11})$$

From Eqs. (B10) and (B11), we now express $\lambda_1(k)$ as a function of k in the limit $k \gg 1$,

$$\lambda_1(k) \simeq k - \frac{\pi^2}{8} + \frac{\pi^2}{4\sqrt{2k}}, \quad (\text{B12})$$

which coincides with the second line of Eq. (28) in the main text. This result gives the asymptotic behavior of the SCGF for the case $N = 1$.

For $N = 2$, we must add the contribution of $\lambda_2(k)$, whose asymptotic behavior in the large- k limit we now calculate. For the second energy level, A_2 goes as $A_2 \rightarrow \frac{\pi^2}{2}$ and by using the corresponding behavior of Eq. (23) and following similar steps as above, we find

$$\lambda_2(k) \simeq k - \frac{\pi^2}{2} + \frac{\pi^2}{\sqrt{2k}}. \quad (\text{B13})$$

Now, using Eqs. (B12) and (B13), we find the asymptotic behavior of the SCGF $\lambda(k) = \lambda_1(k) + \lambda_2(k)$ at $k \rightarrow \infty$,

$$\lambda(k) \simeq 2k - \frac{5\pi^2}{8} + \frac{5\pi^2}{4} \frac{1}{\sqrt{2k}}, \quad (\text{B14})$$

which coincides with Eq. (37) in Sec. IV. We now calculate the Legendre transform of this expression to find the corresponding asymptotic behavior of the rate function. Taking the derivative of Eq. (B14) with respect to k , we get the limiting behavior of $\rho \rightarrow 2$ as

$$\rho = \frac{d\lambda(k)}{dk} = 2 - \frac{5\pi^2}{8\sqrt{2}k^{3/2}}. \quad (\text{B15})$$

By combining Eqs. (B14) and (B15), we find the behavior of the rate function in the limit $\rho \rightarrow 2$,

$$I(\rho) = k\rho - \lambda(k) \simeq \frac{5\pi^2}{8} - 3\left(\frac{5\pi^2}{8\sqrt{2}}\right)^{2/3} (2 - \rho)^{1/3}, \quad (\text{B16})$$

which coincides with Eq. (38) in Sec. IV. The second line of Eq. (29) (for the case $N = 1$) is obtained similarly, by calculating the Legendre transform of Eq. (B12).

-
- [1] T. Bodineau and B. Derrida, Current Fluctuations in Nonequilibrium Diffusive Systems: An Additivity Principle, *Phys. Rev. Lett.* **92**, 180601 (2004).
- [2] R. J. Harris, A. Rákos, and G. M. Schütz, Current fluctuations in the zero-range process with open boundaries, *J. Stat. Mech.* (2005) P08003.
- [3] B. Derrida, Non-equilibrium steady states: fluctuations and large deviations of the density and of the current, *J. Stat. Mech.* (2007) P07023.
- [4] O. Ovaskainen and B. Meerson, Stochastic models of population extinction, *Trends Ecol. Evol.* **25**, 643 (2010).
- [5] N. Merhav and Y. Kafri, Bose-Einstein condensation in large deviations with applications to information systems, *J. Stat. Mech.* (2010) P02011.
- [6] O. Cohen and D. Mukamel, Phase Diagram and Density Large Deviations of a Nonconserving ABC Model, *Phys. Rev. Lett.* **108**, 060602 (2012).

- [7] L. Bertini, A. De Sole, D. Gabrielli, G. Jona-Lasinio, and C. Landim, Macroscopic fluctuation theory, *Rev. Mod. Phys.* **87**, 593 (2015).
- [8] M. Assaf and B. Meerson, WKB theory of large deviations in stochastic populations, *J. Phys. A: Math. Theor.* **50**, 263001 (2017).
- [9] S. S. Varadhan, *Large Deviations and Applications*, CBMS-NSF Regional Conference Series in Applied Mathematics Vol. 46 (SIAM, Philadelphia, 1984).
- [10] R. S. Ellis, *Entropy, Large Deviations, and Statistical Mechanics* (Springer, New York, 1985).
- [11] Y. Oono, Large deviation and statistical physics, *Prog. Theor. Phys. Suppl.* **99**, 165 (1989).
- [12] A. Dembo and O. Zeitouni, *Large Deviations Techniques and Applications*, 2nd ed. (Springer, New York, 1998).
- [13] F. den Hollander, *Large Deviations*, Fields Institute Monographs Vol. 14 (AMS, Providence, Rhode Island, 2000).
- [14] H. Touchette, The large deviation approach to statistical mechanics, *Phys. Rep.* **478**, 1 (2009).
- [15] R. L. Jack, Ergodicity and large deviations in physical systems with stochastic dynamics, *Eur. Phys. J. B* **93**, 74 (2020).
- [16] T. Bodineau and B. Derrida, Distribution of current in nonequilibrium diffusive systems and phase transitions, *Phys. Rev. E* **72**, 066110 (2005).
- [17] J. P. Garrahan, R. L. Jack, V. Lecomte, E. Pitard, K. van Duijvendijk, and F. van Wijland, Dynamical First-Order Phase Transition in Kinetically Constrained Models of Glasses, *Phys. Rev. Lett.* **98**, 195702 (2007).
- [18] G. Bunin, Y. Kafri, and D. Podolsky, Non-differentiable large-deviation functionals in boundary-driven diffusive systems, *J. Stat. Mech.* (2012) L10001.
- [19] C. P. Espigares, P. L. Garrido, and P. I. Hurtado, Dynamical phase transition for current statistics in a simple driven diffusive system, *Phys. Rev. E* **87**, 032115 (2013).
- [20] Y. Baek and Y. Kafri, Singularities in large deviation functions, *J. Stat. Mech.* (2015) P08026.
- [21] Y. Baek, Y. Kafri, and V. Lecomte, Dynamical Symmetry Breaking and Phase Transitions in Driven Diffusive Systems, *Phys. Rev. Lett.* **118**, 030604 (2017).
- [22] Y. Baek, Y. Kafri, and V. Lecomte, Dynamical phase transitions in the current distribution of driven diffusive channels, *J. Phys. A: Math. Theor.* **51**, 105001 (2018).
- [23] T. Nemoto, É. Fodor, M. E. Cates, R. L. Jack, and J. Tailleur, Optimizing active work: Dynamical phase transitions, collective motion, and jamming, *Phys. Rev. E* **99**, 022605 (2019).
- [24] G. Carugno, P. Vivo, and F. Coghi, Delocalization-localization dynamical phase transition of random walks on graphs, *Phys. Rev. E* **107**, 024126 (2023).
- [25] I. Dornic and C. Godrèche, Large deviations and nontrivial exponents in coarsening systems, *J. Phys. A: Math. Gen.* **31**, 5413 (1998).
- [26] J.-M. Drouffe and C. Godrèche, Stationary definition of persistence for finite-temperature phase ordering, *J. Phys. A: Math. Gen.* **31**, 9801 (1998).
- [27] A. Baldassarri, J. P. Bouchaud, I. Dornic, and C. Godrèche, Statistics of persistent events: An exactly soluble model, *Phys. Rev. E* **59**, R20 (1999).
- [28] J.-P. Bouchaud and M. Potters, *Theory of Financial Risk and Derivative Pricing: From Statistical Physics to Risk Management*, 2nd ed. (Cambridge University Press, Cambridge, 2000).
- [29] A. Montanari and R. Zecchina, Optimizing Searches via Rare Events, *Phys. Rev. Lett.* **88**, 178701 (2002).
- [30] V. Kishore, M. S. Santhanam, and R. E. Amritkar, Extreme events and event size fluctuations in biased random walks on networks, *Phys. Rev. E* **85**, 056120 (2012).
- [31] P. Lévy, On certain homogeneous stochastic processes, *Compos. Math.* **7**, 283 (1940).
- [32] M. Kac, On distributions of certain Wiener functionals, *Trans. Am. Math. Soc.* **65**, 1 (1949).
- [33] D. A. Darling and M. Kac, On occupation times for Markoff processes, *Trans. Amer. Math. Soc.* **84**, 444 (1957).
- [34] C. Godrèche and J. M. Luck, Statistics of the occupation time of renewal processes, *J. Stat. Phys.* **104**, 489 (2001).
- [35] S. N. Majumdar and A. Comtet, Local and Occupation Time of a Particle Diffusing in a Random Medium, *Phys. Rev. Lett.* **89**, 060601 (2002).
- [36] G. Bel and E. Barkai, Weak Ergodicity Breaking in the Continuous-Time Random Walk, *Phys. Rev. Lett.* **94**, 240602 (2005).
- [37] E. Barkai, Residence time statistics for normal and fractional diffusion in a force field, *J. Stat. Phys.* **123**, 883 (2006).
- [38] S. Burov and E. Barkai, Occupation Time Statistics in the Quenched Trap Model, *Phys. Rev. Lett.* **98**, 250601 (2007).
- [39] F. D. Stefani, J. P. Hoogenboom, and E. Barkai, Beyond quantum jumps: Blinking nano-scale light emitters, *Phys. Today* **62**(2), 34 (2009).
- [40] O. Bénichou and J. Desbois, Exit and occupation times for Brownian motion on graphs with general drift and diffusion constant, *J. Phys. A: Math. Theor.* **42**, 015004 (2009).
- [41] S. Burov and E. Barkai, Residence Time Statistics for N Renewal Processes, *Phys. Rev. Lett.* **107**, 170601 (2011).
- [42] O. Bénichou and J. Desbois, Occupation times for single-file diffusion, *J. Stat. Mech.* (2015) P03001.
- [43] P. Tsobgni Nyawo and H. Touchette, A minimal model of dynamical phase transition, *Europhys. Lett.* **116**, 50009 (2016).
- [44] P. T. Nyawo and H. Touchette, Dynamical phase transition in drifted Brownian motion, *Phys. Rev. E* **98**, 052103 (2018).
- [45] T. Agranov, P. L. Krapivsky, and B. Meerson, Occupation-time statistics of a gas of interacting diffusing particles, *Phys. Rev. E* **99**, 052102 (2019).
- [46] M. Kimura and T. Akimoto, Occupation time statistics of the fractional Brownian motion in a finite domain, *Phys. Rev. E* **106**, 064132 (2022).
- [47] Z. Toroczka, T. J. Newman, and S. Das Sarma, Sign-time distributions for interface growth, *Phys. Rev. E* **60**, R1115 (1999).
- [48] G. Messin, J. P. Hermier, E. Giacobino, P. Desbiolles, and M. Dahan, Bunching and antibunching in the fluorescence of semiconductor nanocrystals, *Opt. Lett.* **26**, 1891 (2001).
- [49] G. H. Weiss and P. P. Calabrese, Occupation times of a CTRW on a lattice with anomalous sites, *Physica A* **234**, 443 (1996).
- [50] M. D. Donsker and S. R. S. Varadhan, Asymptotics of Wiener sausage, *Commun. Pure Appl. Math.* **28**, 1 (1975).

- [51] M. D. Donsker and S. R. S. Varadhan, On the principal eigenvalue of second-order elliptic differential operators, *Commun. Pure Appl. Math.* **29**, 389 (1976).
- [52] S. N. Majumdar and A. J. Bray, Large-deviation functions for nonlinear functionals of a Gaussian stationary Markov process, *Phys. Rev. E* **65**, 051112, (2002).
- [53] S. N. Majumdar, Brownian functionals in physics and computer science, *Curr. Sci.* **89**, 2076 (2005).
- [54] N. R. Smith, Large deviations in chaotic systems: Exact results and dynamical phase transition, *Phys. Rev. E* **106**, L042202 (2022).
- [55] R. Graham and T. Tél, Existence of a Potential for Dissipative Dynamical Systems, *Phys. Rev. Lett.* **52**, 9 (1984).
- [56] P.-G. de Gennes, Soluble model for fibrous structures with steric constraints, *J. Chem. Phys.* **48**, 2257 (1968).
- [57] M. E. Fisher, Walks, walls, wetting, and melting, *J. Stat. Phys.* **34**, 667 (1984).
- [58] J. W. Essam and A. J. Guttmann, Vicious walkers and directed polymer networks in general dimensions, *Phys. Rev. E* **52**, 5849 (1995).
- [59] A. J. Bray and K. Winkler, Vicious walkers in a potential, *J. Phys. A: Math. Gen.* **37**, 5493 (2004).
- [60] G. Schehr, S. N. Majumdar, A. Comtet, and J. Randon-Furling, Exact Distribution of the Maximal Height of p Vicious Walkers, *Phys. Rev. Lett.* **101**, 150601 (2008).
- [61] G. Schehr, Extremes of N vicious walkers for large N : Application to the directed polymer and KPZ interfaces, *J. Stat. Phys.* **149**, 385 (2012).
- [62] G. Schehr, S. N. Majumdar, A. Comtet, and P. J. Forrester, Reunion probability of N vicious walkers: Typical and large fluctuations for large N , *J. Stat. Phys.* **150**, 491 (2013).
- [63] G. B. Nguyen and D. Remenik, Extreme statistics of non-intersecting Brownian paths, *Electron. J. Probab.* **22**, 1 (2017).
- [64] T. Gautié, P. Le Doussal, S. N. Majumdar, and G. Schehr, Non-crossing Brownian paths and Dyson Brownian motion under a moving boundary, *J. Stat. Phys.* **177**, 752 (2019).
- [65] T. Gautié and N. R. Smith, Constrained non-crossing Brownian motions, fermions and the Ferrari-Spohn distribution, *J. Stat. Mech.* (2021) 033212.
- [66] J. Grela, S. N. Majumdar, and G. Schehr, Non-intersecting Brownian bridges in the flat-to-flat geometry, *J. Stat. Phys.* **183**, 49 (2021).
- [67] F. J. Dyson, A Brownian-motion model for the eigenvalues of a random matrix, *J. Math. Phys.* **3**, 1191 (1962).
- [68] K. Johansson, From Gumbel to Tracy-Widom, *Probab. Theory Relat. Fields* **138**, 75 (2007).
- [69] M. Katori, Determinantal process starting from an orthogonal symmetry is a Pfaffian process, *J. Stat. Phys.* **146**, 249 (2012).
- [70] We emphasize that the process that we consider is N Brownian motions conditioned not to cross each other. This is not be confused with a hard-core repulsion between the particles. The latter would result in reflecting boundary conditions, instead of the absorbing boundary conditions (14) for the noncrossing case.
- [71] J. Gärtner, On large deviations from the invariant measure, *Theory Probab. Appl.* **22**, 24 (1977).
- [72] R. S. Ellis, Large deviations for a general class of random vectors, *Ann. Probab.* **12**, 1 (1984).
- [73] H. Touchette, Legendre-Fenchel transforms in a nutshell, <https://www.ise.ncsu.edu/fuzzy-neural/wp-content/uploads/sites/9/2019/01/or706-LF-transform-1.pdf> (2005).
- [74] D. A. Huse and M. E. Fisher, Commensurate melting, domain walls, and dislocations, *Phys. Rev. B* **29**, 239 (1984).
- [75] C. Krattenthaler, A. J. Guttmann, and X. G. Viennot, Vicious walkers, friendly walkers and Young tableaux: II. With a wall, *J. Phys. A: Math. Gen.* **33**, 8835 (2000).
- [76] H. Touchette, Introduction to dynamical large deviations of Markov processes, *Physica A* **504**, 5 (2018).
- [77] D. J. Griffiths, *Introduction to Quantum Mechanics*, 2nd ed. (Cambridge University Press, Cambridge, 2005).
- [78] B. C. Hall, *Quantum Theory for Mathematicians* (Springer, New York, NY, 2013).
- [79] The absence of the usual normalization factor $1/\sqrt{N!}$ before the Slater determinant in Eq. (31) is because it is constrained to $X_1 < \dots < X_N$ in contrast to the usual case with fermions, thus leading to a different normalization factor.
- [80] D. S. Dean, P. Le Doussal, S. N. Majumdar, G. Schehr, and N. R. Smith, Kernels for noninteracting fermions via a Green's function approach with applications to step potentials, *J. Phys. A: Math. Theor.* **54**, 084001 (2021).
- [81] Y. Castin, Simple theoretical tools for low dimension Bose gases, *J. Phys. IV France* **116**, 89 (2004).
- [82] P. Calabrese, M. Mintchev, and E. Vicari, Exact relations between particle fluctuations and entanglement in Fermi gases, *Europhys. Lett.* **98**, 20003 (2012).
- [83] V. Eisler, Universality in the Full Counting Statistics of Trapped Fermions, *Phys. Rev. Lett.* **111**, 080402 (2013).
- [84] R. Marino, S. N. Majumdar, G. Schehr, and P. Vivo, Phase Transitions and Edge Scaling of Number Variance in Gaussian Random Matrices, *Phys. Rev. Lett.* **112**, 254101 (2014).
- [85] D. S. Dean, P. Le Doussal, S. N. Majumdar, and G. Schehr, Noninteracting fermions at finite temperature in a d -dimensional trap: Universal correlations, *Phys. Rev. A* **94**, 063622 (2016).
- [86] I. Bloch, J. Dalibard, and W. Zwerger, Many-body physics with ultracold gases, *Rev. Mod. Phys.* **80**, 885 (2008).
- [87] L. W. Cheuk, M. A. Nichols, M. Okan, T. Gersdorf, R. Vinay, W. Bakr, T. Lompe, and M. Zwierlein, Quantum-Gas Microscope for Fermionic Atoms, *Phys. Rev. Lett.* **114**, 193001 (2015).
- [88] E. Haller, J. Hudson, A. Kelly, D. A. Cotta, B. Peaudecerf, G. D. Bruce, and S. Kuhr, Single-atom imaging of fermions in a quantum-gas microscope, *Nat. Phys.* **11**, 738 (2015).
- [89] M. F. Parsons, F. Huber, A. Mazurenko, C. S. Chiu, W. Setiawan, K. Wooley-Brown, S. Blatt, and M. Greiner, Site-Resolved Imaging of Fermionic ${}^6\text{Li}$ in an Optical Lattice, *Phys. Rev. Lett.* **114**, 213002 (2015).
- [90] B. Mukherjee, Z. Yan, P. B. Patel, Z. Hadzibabic, T. Yefsah, J. Struck, and M. W. Zwierlein, Homogeneous Atomic Fermi Gases, *Phys. Rev. Lett.* **118**, 123401 (2017).
- [91] M. Holten, L. Bayha, K. Subramanian, C. Heintze, P. M. Preiss, and S. Jochim, Observation of Pauli Crystals, *Phys. Rev. Lett.* **126**, 020401 (2021).

- [92] P. Calabrese, P. Le Doussal, and S. N. Majumdar, Random matrices and entanglement entropy of trapped Fermi gases, *Phys. Rev. A* **91**, 012303 (2015).
- [93] D. S. Dean, P. Le Doussal, S. N. Majumdar, and G. Schehr, Noninteracting fermions in a trap and random matrix theory, *J. Phys. A: Math. Theor.* **52**, 144006 (2019).
- [94] N. R. Smith, P. Le Doussal, S. N. Majumdar, and G. Schehr, Full counting statistics for interacting trapped fermions, *SciPost Phys.* **11**, 110 (2021).
- [95] The \sum in Eq. (A5) is to be understood as a sum over the discrete part of the spectrum of the tilted operator plus an integral over the continuous part of the spectrum.